A Method for Achieving Electromagnetic Wave Absorption by Low-Loss Stratified Construction Materials

Nozomu Ishii, *Member, IEEE*, Michio Miyakawa, *Member, IEEE*, and Koji Sakai

***Abstract*—For the safe and effective use of electromagnetic waves, a method for designing construction materials having selective electromagnetic wave absorption is needed. As an example, the characteristics of a stratified construction material consisting of two different low-loss materials (acrylic resin and glass) is evaluated by numerical simulation, and the electromagnetic wave absorption mechanism is determined. Furthermore, a method is developed for designing stratified construction materials to realize electromagnetic wave absorption at a desired frequency.**

***Index Terms*—Construction material, cutoff frequency, electromagnetic absorption, low-loss material, nonradiative dielectric waveguide, stratified media.**

I. Introduction

THE OPTIMIZED design of electromagnetic (EM) wave absorption in living spaces, is important for the safe and effective use of EM waves. For this reason, new construction materials will be used to intercept EM waves at specific frequencies while permitting transmission of other wave components into the living space. However, the materials and living spaces constructed of those materials need to be available at reasonable cost. Of course, complete shielding is feasible, for example, by covering the target space in RF absorber or a metal enclosure. However, the goal is to obtain the desired EM wave absorption characteristics within a specified space by using new construction materials, fabricated by combining two or more materials and adjusting the spatial configuration [1]–[3]. As an example of these materials, we focus on a stratified construction material consisting of two low-loss parallel slabs or two material boards laminated with an oblique boundary [3]. Through two-dimensional (2-D) transverse magnetic (TM) finite-difference time-domain (FDTD) simulation, characteristics of the frequency dependent EM wave absorption were analyzed by evaluating the EM wave absorption ratio at the back of the material. By introducing an equivalent dielectric constant, reflection/transmission of EM waves from the stratified construction material for normal incident TM polarization was analyzed. From the computed results, the stratified material was demonstrated to exhibit selective absorption characteristics. In addition to the analysis, a method for designing selective absorption was established.

Manuscript received June 24, 2002; revised July 15, 2004. This work was supported in part by the Japan Society for the Promotion of Science (JSPS) under Grant (B)(1)11490011.

N. Ishii and M. Miyakawa are with the Faculty of Engineering, Niigata University, Niigata 950 2181, Japan.

K. Sakai is with the Advantest Corporation, Tokyo 100 0005, Japan.

Digital Object Identifier 10.1109/TEMC.2004.842105

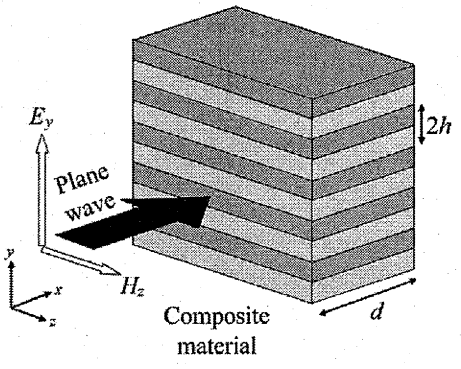

Fig. 1. Composite construction material consisting of alternating layers.

The proposed absorbing materials may have the limits that the absorption is not very large and its bandwidth is very narrow, from a conventional EMC perspective. In general, there are some methods to realize the EM wave shielding and absorption, for example, to absorb the EM wave with absorbing materials or shield it with matallic enclosure and to block the EM wave with spatial filtering or FSS (frequency selective surface). In this paper, we propose the new method for the EM wave absorption which occurs at the cutoff frequency of the higher modes generated on the interface of two materials. In addition, the possibility and the principle of the sharp absorption are clarified. The proposed absorbing material is useful for reducing the emission of the EM wave into surrounding area at a lower cost, for example, in the transmitting wireless system, to strengthen the shielding or the absorption by the conventional methods. Moreover, the merit of the proposed method is that the absorbing materials can be composed of the construction materials with low loss, which are not more expensive than the conventional absorbers.

II. FDTD Analysis of Stratified Construction Material

A. Numerical Model and Analytical Conditions

As shown in Fig. 1, we assume a layered composite material consisting of two low-loss construction materials having different dielectric constants. The composite material has a periodical structure with a period of $2h$ in the y direction, thickness of d in the x direction, and spreads infinitely in the z direction. An analytic model of the structure is shown in Fig. 2. Only half a period of the stratified materials is sandwiched by

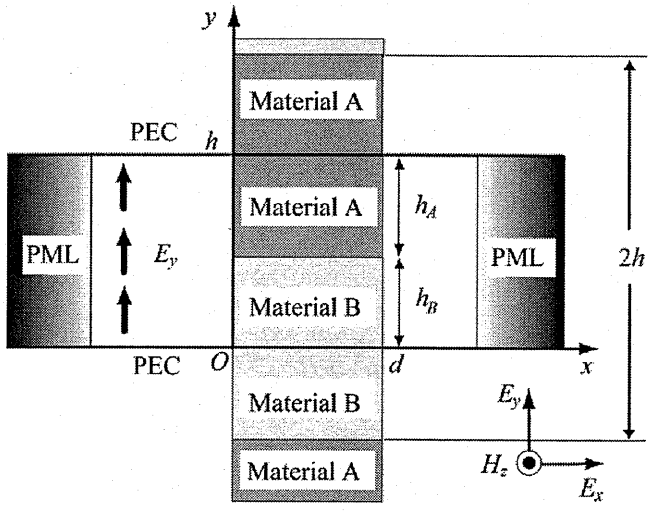

Fig. 2. Equivalent model using electric walls (PECs).

TABLE I
DIELECTRIC CONSTANT AND CONDUCTIVITY OF MATERIALS AT 1.5 GHz

	Material	ε_r	σ[S/m]
A	Acrylic resin	$\varepsilon_A = 2.6$	0.002
B	Glass	$\varepsilon_B = 5.2$	0.002

two electric walls a distance apart h. To examine EM wave absorption by the material, the equivalent model in Fig. 2 was numerically analyzed using 2-D TM FDTD techniques. Materials A ($h_B < y < h$) and B ($0 < y < h_B$) are assumed to be acrylic resin and glass, respectively. The dielectric constant and conductivity of acrylic resin and glass at 1.5 GHz are listed in Table I [4]. These values are assumed to be constant over the frequency range used in the numerical analysis. Berenger's PML absorbing boundary condition (16 layers) [5] is built into our FDTD code. As shown in Fig. 1, when the plane wave excited by a Gaussian pulse is incident normally onto the surface of the material, the reflected power P_r is calculated at $x = -100$ mm in front of the material and the transmitted power P_t is calculated at $x = d + 100$ mm from the back of the material. Power loss in the composite material P_l is then given by

$$P_l = P_i - P_r - P_t \tag{1}$$

where P_i is the input power, which can be estimated from P_t with no material. The frequency range is limited to below 5 GHz because mobile communication EM wave sources are assumed in this analysis.

B. Results of FDTD-Based Computation

1) $d = 150$ mm, $h_A = h_B = 20$ mm: Reflectivity P_r/P_i, the transmissivity P_t/P_i, and the absorption ratio P_l/P_i are shown in Fig. 3, for $d = 150$ mm and $h_A = h_B = 20$ mm. The reflectivity and transmissivity can be seen to have a periodicity with a certain frequency interval, due to the standing wave produced in the material. We call the frequencies at which steep absorption occurs "absorbing peak frequency." It is observed that the absorption ratio is almost constant across the frequency range of interest, as shown in Fig. 3. The absorbing peak frequencies exist discretely, for example, at 1.93, 2.12, 2.40, ... GHz (also see Table IV). At the absorbing peak frequencies, the reflectivity and transmissivity are relatively small, as shown in Fig. 3. At the first peak frequency of 1.935 GHz, the reflectivity, transmitivity, and absorption ratio become −21.0 dB, −3.1 dB, and −4.2 dB, respectively, when $h_A = h_B = 20$ mm and $d = 150$ mm. Although the absorption is not complete, 38.4% of the input power is dissipated in the composite material, and the bandwidth of the absorbing peak at 1.935 GHz is very narrow, about 1.0%–1.5% of the peak frequency.

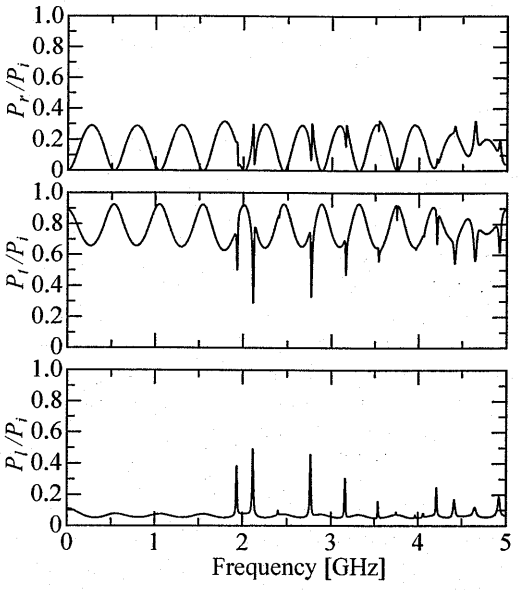

Fig. 3. Power balance for the periodic structure of Fig. 2, where $h_A = h_B = 20$ mm, $d = 150$ mm.

TABLE II
RELATIONSHIP BETWEEN f_{p1} AND P_r/P_i, P_t/P_i, P_l/P_i FOR $d = 150$ mm, $h = h_A + h_B = 40$ mm

$h_A : h_B$	f_{p1}[GHz]	P_r/P_i	P_t/P_i	P_l/P_i
1 : 3	1.747	0.229	0.477	0.294
1 : 1	1.935	0.123	0.493	0.384
3 : 1	2.268	0.008	0.775	0.217

2) $d = 150$ mm, $h = h_A = h_B$ is Varied: According to the composite ratio of the materials $h_A : h_B$, the computed first absorbing peak frequency f_{p1} and absorption ratio P_l/P_i vary as shown in Table II, when $d = 150$ mm and $h = h_A + h_B = 40$ mm. To reduce the absorbing peak frequency, the volume of acrylic resin has to be larger than that of glass, i.e., the equivalent dielectric constant needs to be larger. The absorption ratio varies with the ratio $h_A : h_B$, and absorption ratio in the case of $h_A : h_B = 1 : 1$ is the largest of the three cases in Table II. The first absorbing peak frequency f_{p1} and absorption ratio at the frequency f_{p1} are plotted against h as shown in Fig. 4, for the ratio $h_A : h_B = 1 : 1$ and $d = 150$ mm. The most suitable h to locally maximize the absorption ratio was found in the range from $h = 20$ mm to $h = 70$ mm.

3) $h_A = h_B = 20$ mm, d is Varied: In Fig. 5, the first absorbing peak frequency f_{p1} and the absorption ratio P_l/P_i are shown as a function of d when $h_A = h_B = 20$ mm. As d is increased, the absorbing peak frequency decreases to about

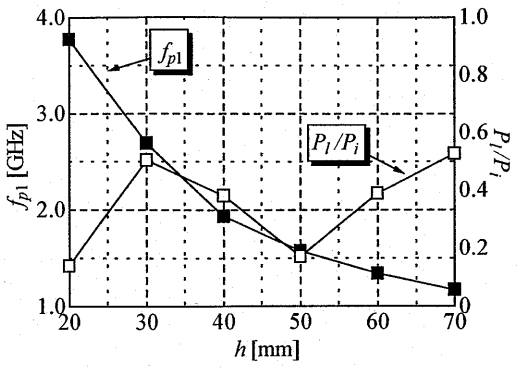

Fig. 4. h versus f_{p1}, P_l/P_i for $h_A : h_B = 1 : 1$, $d = 150$ mm.

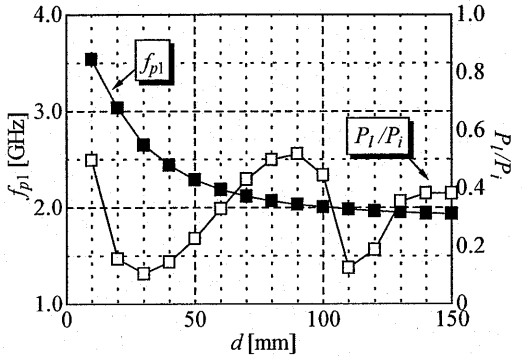

Fig. 5. d versus f_{p1}, P_l/P_i for $h_A = h_B = 20$ mm.

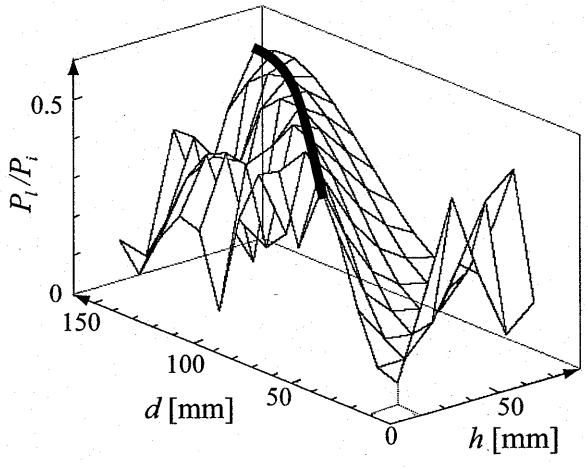

Fig. 6. Value of P_l/P_i at f_{p1} for various values of d and h, where $h_A : h_B = 1 : 1$.

1.93 GHz, which is the lowest limit. A most suitable d for maximizing P_l/P_i locally in the range below $d = 150$ mm is thought to exist.

4) P_l/P_i Versus h, When $h = h_A + h_B$ is Varied: When both h and d were varied while maintaining the relation $h_A : h_B = 1 : 1$, the absorption ratio P_l/P_i varied as shown in Fig. 6. The thick line shows the locus of points for which the ratio P_l/P_i is maintained at higher values. This gives the dependence of material thickness on absorption ratio.

5) $d = 150$ mm, $h_A = h_B = 20$ mm, σ is Varied: The frequency characteristics of P_l/P_i for two materials having various conductivities, σ are shown in Fig. 7 for $d = 150$ mm and

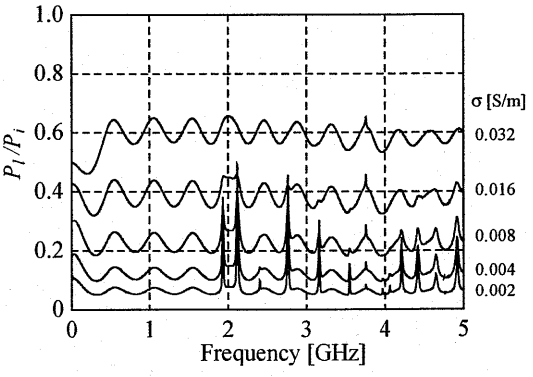

Fig. 7. Frequency versus P_l/P_i for various values of conductivity σ, where $d = 150$ mm, $h_A = h_B = 20$ mm.

$h_A = h_B = 20$ mm. Absorption ratio P_l/P_i is clearly almost in proportion to conductivity σ. However, the sharp absorption characteristics tend to disappear as conductivity increases. Low-loss materials are concluded to be needed to realize these sharp absorption characteristics.

C. Mechanism of Steep Loss

With reference to the case of $d = 150$ mm and $h_A = h_B = 20$ mm, the mechanism of the steep loss observed in Figs. 3 and 7 is discussed. When a plane wave is incident normally on the material surface, an electric field component E_x is produced at the boundary to satisfy the boundary condition [6]. However, this electric field cannot couple to the transmitted transverse electromagnetic (TEM) mode in the materials. For the higher modes that can be supported in the materials (TM_{mn} modes), the E_x produced at the boundary can couple to these higher modes to support the E_x along the boundary between the two materials. Below the cutoff frequency of the higher modes, E_x along the boundary does not exist. However, at the cutoff frequency at which higher modes begin to be supported, the EM wave resonates in a direction perpendicular to the propagating direction, but does not propagate. This resonance occurs in the periodical direction, and the electric field intensity in the materials $|\mathbf{E}|$ is large. Therefore, the power loss in the materials

$$P_l = \frac{\sigma}{2} \iint_{S_2} |\mathbf{E}|^2 dS \tag{2}$$

is large, where S_2 is the cross-section of Region 2. Steady-state $|E_x|$ distributions at 1.93 GHz and 2.02 GHz obtained by FDTD-based computation are shown in Fig. 8(a) and (b), respectively. These frequencies correspond to in and out of resonance, respectively. From the figure, E_x clearly exhibits a resonance at 1.93 GHz, as can also be seen by the sharp absorption in Fig. 3.

A major source of loss in the materials is the E_y excited when a plane wave passes through the materials. In contrast, absorption peak frequency is determined by the excited E_x, which is parallel to the boundary surface and exhibits resonance characteristics in the y direction. Sharp absorption characteristics are not observed if the power loss by resonance becomes equal to or less than that of plane wave propagation. This is the reason for the steep absorption disappearing as conductivity increases.

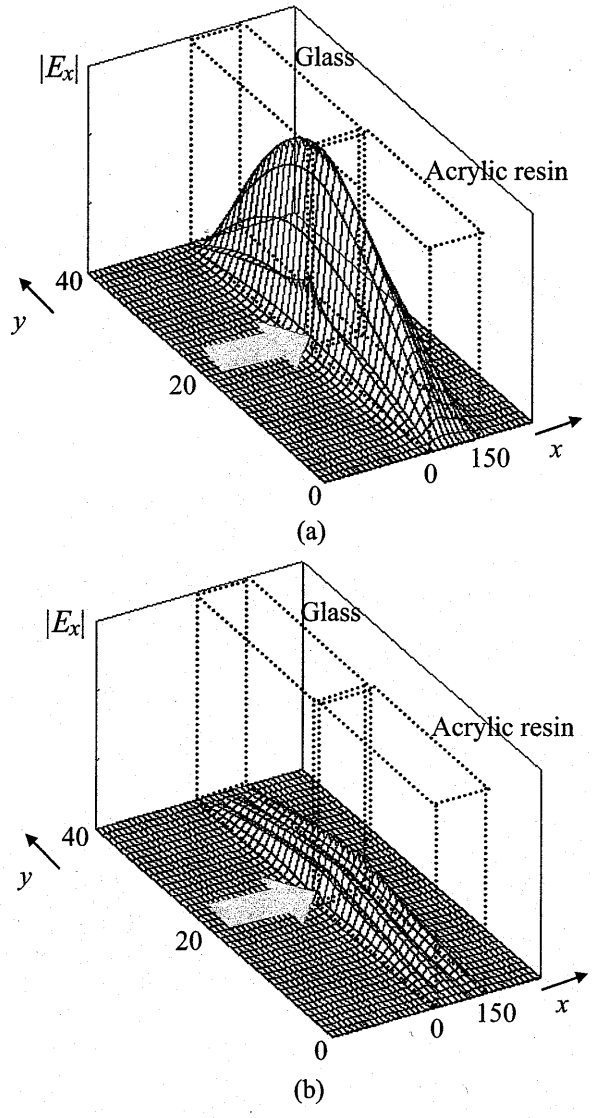

Fig. 8. $|E_x|$ distribution at the frequencies corresponding to sharp and normal absorption. (a) 1.93 GHz (at resonance). (b) 2.02 GHz (off resonance).

The absorption ratios from Figs. 3–5 are not necessarily large enough, but it is increased by using slanted joining dielectrics instead of the stratified ones. For example, the absorption ratio of 77% is easily obtained according to the FDTD calculation [3]. Therefore, the material with a high absorption ratio is obtainable. It will be feasible to produce absorbing materials which show a high absorption ratio in a wider frequency range by combining appropriate raw materials with various shapes and sizes.

III. Analytical Consideration of Stratified Construction Material

The absorption ratio of the materials has been analytically estimated using an equivalent model, as shown in Fig. 2. We first introduce an equivalent dielectric constant ε_e to replace the model by a simplified model consisting of an equivalent medium. For the modes which are supported in the simplified model, we analyze the reflection/transmission of EM waves in the equivalent medium.

TABLE III
$h_A : h_B$ VERSUS EQUIVALENT DIELECTRIC CONSTANT ε_e FOR $\varepsilon_A = 2.6, \varepsilon_B = 5.2$

$h_A : h_B$	3 : 1	1 : 1	1 : 3
ε_e	3.25	3.90	4.55

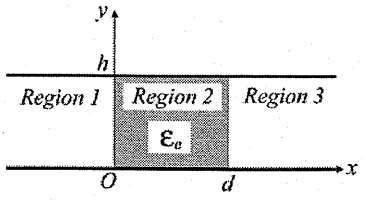

Fig. 9. Equivalent model using an equivalent dielectric constant.

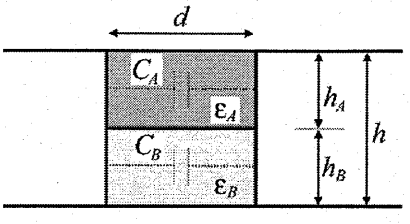

Fig. 10. Equivalent circuit representation of the material region.

A. Equivalent Dielectric Constant

An equivalent circuit for the material region (Region 2) is shown in Fig. 10. C_A and C_B denote the capacitances per unit length of material A and B, respectively. The total capacitance per unit length for material C is then given by

$$C = \varepsilon_e\varepsilon_0\frac{(h_A+h_B)\cdot 1}{d} = C_A + C_B = \varepsilon_A\varepsilon_0\frac{h_A\cdot 1}{d} + \varepsilon_B\varepsilon_0\frac{h_B\cdot 1}{d} \tag{3}$$

using the static formula for the capacitance of a parallel plate capacitor. From (3), the equivalent dielectric constant is given by

$$\varepsilon_e = \frac{\varepsilon_A h_A + \varepsilon_B h_B}{h_A + h_B}. \tag{4}$$

For the stratified structure consisting of acrylic resin and glass, the equivalent dielectric constant ε_e is calculated for various ratios of h_A to h_B, as shown in Table III. From (4), the equivalent dielectric constant ε_e is independent of the thickness d of the material.

B. Formulation of Reflection/Transmission in the Material

As shown in Fig. 9, an EM wave is incident normally onto the material surface from Region 1 (free space, $x \leq 0$), and reflected and transmitted waves are produced in Region 2 (material, $0 \leq x \leq d$). Only a transmitted wave exists in Region 3 (free space, $x \geq d$). TM_{mn} mode EM waves that support a parallel electric field E_x are acceptable as incident waves. The wavenumber in the y direction k_{yn} and the phase constant β_n^a, β_n^d are given by

$$k_{yn} = \frac{n\pi}{h} \tag{5}$$

$$\beta_n^a = \sqrt{k_0^2 - k_{yn}^2} \quad \beta_n^d = \sqrt{\varepsilon_e k_0^2 - k_{yn}^2} \tag{6}$$

where $k_0 = \omega\sqrt{\mu_0\varepsilon_0} = \omega/c$ is the wavenumber in free space and c is the velocity of light. In (6), the superscripts a and d represent air and dielectric regions, respectively. The EM fields in each region can be expanded by using modal functions for the TM_n mode lossless parallel plate waveguide [7].

Region 1

$$E_{x,n}^{(1)} = \left(e^{-j\beta_n^a x} + \Gamma_n^{(1)} e^{j\beta_n^a x}\right) \sin k_{yn} y \tag{7}$$

$$E_{y,n}^{(1)} = \frac{j\beta_n^a}{k_{yn}} \left(-e^{-j\beta_n^a x} + \Gamma_n^{(1)} e^{j\beta_n^a x}\right) \cos k_{yn} y \tag{8}$$

$$H_{z,n}^{(1)} = \frac{j\omega\varepsilon_0}{k_{yn}} \left(e^{-j\beta_n^a x} + \Gamma_n^{(1)} e^{j\beta_n^a x}\right) \cos k_{yn} y. \tag{9}$$

Region 2

$$E_{x,n}^{(2)} = \left(T_n^{(2)} e^{-j\beta_n^d x} + \Gamma_n^{(2)} e^{j\beta_n^d x}\right) \sin k_{yn} y \tag{10}$$

$$E_{y,n}^{(2)} = \frac{j\beta_n^d}{k_{yn}} \left(-T_n^{(2)} e^{-j\beta_n^d x} + \Gamma_n^{(2)} e^{j\beta_n^d x}\right) \cos k_{yn} y \tag{11}$$

$$H_{z,n}^{(2)} = \frac{j\omega\varepsilon_0\varepsilon_e}{k_{yn}} \left(T_n^{(2)} e^{-j\beta_n^d x} + \Gamma_n^{(2)} e^{j\beta_n^d x}\right) \cos k_{yn} y. \tag{12}$$

Region 3

$$E_{x,n}^{(3)} = \left(T_n^{(3)} e^{-j\beta_n^a x}\right) \sin k_{yn} y \tag{13}$$

$$E_{y,n}^{(3)} = \frac{j\beta_n^a}{k_{yn}} \left(-T_n^{(3)} e^{-j\beta_n^a x}\right) \cos k_{yn} y \tag{14}$$

$$H_{z,n}^{(3)} = \frac{j\omega\varepsilon_0}{k_{yn}} \left(T_n^{(3)} e^{-j\beta_n^a x}\right) \cos k_{yn} y. \tag{15}$$

$\Gamma_n^{(1)}$ is the reflection coefficient for the reflected wave in Region1, $\Gamma_n^{(2)}$ is the coefficient for the reflected wave in Region 2, $T_n^{(2)}$ is the coefficient for the transmitted wave in Region 2, and $T_n^{(3)}$ is the transmission coefficient for the transmitted wave in Region 3. The modal functions are selected to satisfy the boundary condition, or continuity of the normal component of electric flux density at $x = 0$ and d. The remaining boundary conditions are

(a) $E_{y,n}^{(1)} = E_{y,n}^{(2)}$, $H_{z,n}^{(1)} = H_{z,n}^{(2)}$ at $x = 0$
(b) $E_{y,n}^{(2)} = E_{y,n}^{(3)}$, $H_{z,n}^{(2)} = H_{z,n}^{(3)}$ at $x = d$.

All of the coefficients can now be determined. Suppose that β_n^d is a positive real number, then the power loss in Region 2, $P_{l,n}^{(2)}$ can be written as

$$P_{l,n}^{(2)} = \frac{\sigma}{2} \iint_{S_2} |\mathbf{E}_n|^2 dS = \frac{2\sigma h |\beta_n^a|^2}{\beta_n^d N_n} \left\{ \left(\frac{\beta_n^d}{k_{yn}}\right)^2 M_n^+ + M_n^- \right\} \tag{16}$$

$$M_n^{\pm} = \left[\left(\beta_n^d\right)^2 + \left(\varepsilon_e |\beta_n^a|\right)^2\right] \left(\beta_n^d d\right) - \sin \beta_n^d d \left\{ \pm \left[\left(\beta_n^d\right)^2 - \left(\varepsilon_e |\beta_n^a|\right)^2\right] \cos \beta_n^d d + 2\varepsilon_e \beta_n^d \mathrm{Im}\left[\beta_n^a\right] \sin \beta_n^d d \right\} \tag{17}$$

TABLE IV
COMPARISON BETWEEN CUTOFF FREQUENCIES FOR LSM_{1m} MODE OF NRDG AND FDTD-BASED ABSORPTION PEAK FREQUENCIES

	Cutoff Frequency [GHz]				
m	1	2	3	4	5
Eqs. (19) or (20)	1.96	2.13	2.38	2.69	3.04
FDTD	1.93	2.12	2.40	2.77	3.16

$$N_n = \left| \left(\beta_n^d + \varepsilon_e \beta_n^a\right)^2 e^{j\beta_n^d d} - \left(\beta_n^d - \varepsilon_e \beta_n^a\right)^2 e^{-j\beta_n^d d} \right|^2 \tag{18}$$

where the symbol Im[ ] is a mathematical operator that selects the imaginary part of a complex quantity. Power loss $P_{l,n}^{(2)}$ exhibits sharp frequency characteristics if N_n in the denominator of (16) vanishes. $N_n = 0$ yields

$$\frac{\varepsilon_e \beta_n^a}{\beta_n^d} = -j \tan\left(\frac{\beta_n^d d}{2}\right) \tag{19}$$

$$\frac{\varepsilon_e \beta_n^a}{\beta_n^d} = j \cot\left(\frac{\beta_n^d d}{2}\right). \tag{20}$$

Equation (19) is the characteristic equation of the odd LSM_{nm} modes of a nonradiative dielectric waveguide (NRDG) [8]. Equation (20) is the characteristic equation of the even LSM_{nm} modes of NRDG. The xy-plane in Fig. 9 corresponds to the cross-section of NRDG. At the frequency where resonance begins, i.e., the cutoff frequency of the higher modes, power loss increases rapidly. The peak frequencies obtained by FDTD analysis in the case of Fig. 2 and cutoff frequencies of NRDG at $n = 1$ calculated by solving (19) and (20) are compared in Table IV.

In summary, we can find the absorbing peak frequency $f_{p,n}$ by introducing an equivalent dielectric constant, as given by (4). By replacing the composite material with an equivalent medium, estimating the cutoff frequency of the corresponding NRDG and solving (19) and (20), we can determine those peak frequencies.

IV. METHOD FOR DESIGNING STRATIFIED CONSTRUCTION MATERIALS

In this section, we describe a method for selecting structural parameters to realize EM wave absorption at a specific frequency in composite construction materials. Equations are derived for determining h and d when the absorbing peak frequency f_p is given. Losses in the materials are ignored because low-loss materials are essential for fabricating the composite materials that have been discussed. From (4), if the composite ratio of materials $h_A : h_B$ is kept constant, the corresponding equivalent dielectric constant ε_e becomes a constant that is independent of d and h. The wavenumber k_0 in (6) is replaced by the following k_p:

$$k_p = \frac{2\pi f_p}{c}. \tag{21}$$

From (6)

$$\beta_n^a = -j\sqrt{k_{yn}^2 - k_p^2} \tag{22}$$

TABLE V
SOLUTION OF EQ. (23) FOR $d = 150$ mm, WHERE $h_A : h_B = 1 : 1, \varepsilon_e = 3.90, f_p = 1.5$ GHz

m	1	2	3
h[mm]	53.3	64.5	92.8

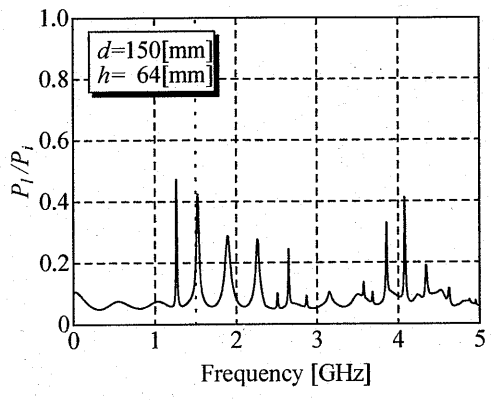

Fig. 11. Frequency versus absorption ratio P_l/P_i for a specified frequency of 1.5 GHz, where $h = 64$ mm, $h_A : h_B = 1 : 1, \varepsilon_A = 2.6, \varepsilon_B = 5.2$.

is obtained. From (19), (20), and (22)

$$d = \frac{2}{\beta_n^d}\left[\frac{(m-1)\pi}{2} + \tan^{-1}\left(\frac{\varepsilon_e\sqrt{k_{yn}^2 - k_p^2}}{\beta_n^d}\right)\right], \quad \text{for } m = 1, 2, \ldots. \tag{23}$$

When m is an odd number, (23) corresponds to (19), i.e., odd LSM_{nm} mode. When m is an even number, (23) corresponds to (20), i.e., even LSM_{nm} mode. The relationship between k_{yn} and h is given by (5) so that (23) is the design equation for determining d and h when the absorbing peak frequency is given.

Firstly, h is chosen so that the absorbing frequency coincides with the desired value. For example, the values of h that satisfy (23) at 1.5 GHz are given in Table V for d equal to 150 mm. Fig. 11 shows the frequency characteristics of absorption ratio P_l/P_i for 64 mm as obtained by FDTD based computation. In this computation, rounded values of h are used due to the cell size in the FDTD analysis. From this figure, the absorbing peak frequency can be seen to have been specified precisely. There are two reasons why the resultant peak frequencies are slightly different from the specified values. One is the difference in h values. That is, the numerical model for FDTD analysis is represented by use of the unit size of a cell, regardless of accuracy of the calculated value for h. Use of an equivalent dielectric instead of two laminated dielectrics may be the second reason.

Secondly, large absorption cannot be obtained if only the parameter h is varied. To discuss this problem further, both h and d need to be determined by (22) over the range of h and d in which the absorption ratio is large (cf. Fig. 6). If h and d are chosen properly, absorbing peak frequency will match the specified frequency well. The relation between d and h for $n = 1$ is shown in Fig. 12 when the peak frequency is set to 1.5 GHz. In the case of $d = 150$ mm, for example, the steep absorption can be seen graphically to be observed at three frequencies corresponding to $m = 1$, 2 and 3 in Table V. Moreover, from the

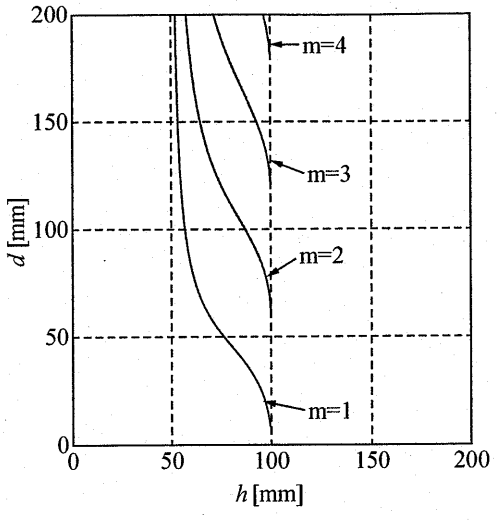

Fig. 12. $h - d$ design diagram for $h_A : h_B = 1 : 1, \varepsilon_A = 2.6, \varepsilon_B = 5.2$.

condition that the argument of the root in (23) has to be zero or positive, h is found to be limited to within the range

$$\frac{\lambda_e}{2} \le h \le \frac{\lambda_0}{2} \tag{24}$$

where $\lambda_e = \lambda_0/\sqrt{\varepsilon_e}$ is the effective wavelength in the material region. The allowable range of h corresponding to Fig. 12 is from 50.6 to 100 mm. This limitation on h must be adhered to. Furthermore, as easily seen from Fig. 12, if d is included in the range

$$(m-1)\Delta d \le d \le m\Delta d \tag{25}$$

steep absorptions occur. From (23), Δd is given by

$$\Delta d = \frac{\pi}{\sqrt{\varepsilon_e k_p^2 - k_{yn}^2}}. \tag{26}$$

For example, Δd is 60.4 mm in the case of Fig. 12.

V. CONCLUSION

In this study, we have demonstrated that relatively large EM wave absorption at a specified frequency can be induced in stratified construction material consisting of two kinds of low-loss materials. Through 2-D TM FDTD analysis, the electric field component that propagates perpendicularly to the incident wave is shown to be produced at the boundary between the two different construction materials. Resonance phenomena occur in the transverse components, which are perpendicular to the direction of propagation. Therefore, relatively large absorption is induced in low-loss materials in which resonance plays an important role.

By introducing an equivalent dielectric constant, the resonance phenomenon was analyzed to determine the relationship between resonant frequency and cutoff frequency of higher modes of a parallel plate waveguide. This was done by solving a boundary problem related to the reflection/transmission of three layers in the parallel plate waveguide. Finally, we found the important relationship and showed that relatively large absorption can be realized at an arbitrary frequency.

In conclusion, we have described a method for designing stratified construction material to induce EM wave absorption at a desired frequency. Up to now, the application of composite materials has been limited because of a narrow bandwidth and incomplete shielding effects. Although the absorption is not so complete as compared to the traditional RF absorber, it is increased by choosing the appropriate shape and sizes of the components (raw materials) or by changing the combination of those components. In transmitting stations for TV broadcast and wireless systems, a few dB absorption of the EM wave can be achieved using composite construction materials. This is useful for reducing the emission of EM waves into the surrounding area at a lower cost.

In this paper, we dealt with the case of a normal incident TM wave impinging on the composite construction material. However, to diminish the incident waves, which can be generated inside the building, we need to include the case of oblique incidence of plane waves of both TM and TE polarizations in our analysis. From this point of view, we will examine the oblique incidence problem in future work.

REFERENCES

[1] M. Miyakawa, M. Kubota, S. Kaneko, N. Ishii, and Y. Kanai, "Permittivity measurement of construction materials for living space design in full consideration of EMC," in *Proc. PIERS'00*, vol. 1, Jul. 2000, p. 24.

[2] M. Miyakawa, M. Shimada, N. Ishii, T. Saeki, and Y. Kanai, "Model-based permittivity measurement of construction materials by the standing wave method," in *Proc. IEEE EMC Int. Symp.*, vol. 2, Aug. 2001, pp. 1135–1140.

[3] M. Miyakawa, K. Sakai, and N. Ishii, "Selective use of EM waves in the closed space constructed by traditional but new construction materials with various surface structure," in *Proc. IEEE EMC Int. Symp.*, vol. 2, Aug. 2001, pp. 794–798.

[4] A. R. von Hippel, Ed., *Table of Dielectric Material*. Cambridge, MA: MIT Press, 1954.

[5] J. P. Berenger, "A perfectly matched layer for the absorption of electromagnetic waves," *J. Com. Phys.*, vol. 114, pp. 185–200, 1994.

[6] H. Sato, H. Domae, M. Takahashi, and M. Abe, "Reflection and transmission control of electromagnetic wave for concrete walls," *Trans. IEICE Japan*, vol. J82-B, no. 4, pp. 674–682, 1999.

[7] D. M. Pozar, *Microwave Engineering*, 2nd ed. New York: Wiley, 1998.

[8] T. Yoneyama and S. Nishida, "Nonradiative dielectric waveguide for millimeter-wave and optical integrate circuits," *IEEE Trans. Microwave Theory Tech.*, vol. MTT-29, no. 11, pp. 1188–1192, Nov. 1981.

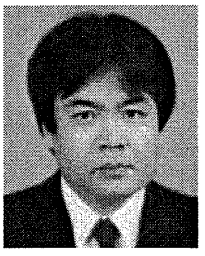

Nozomu Ishii (S'92–M'92) was born in Sapporo, Japan, in 1966. He received the B.S., M.S., and Ph.D. degrees from Hokkaido University, Sapporo, Japan, in 1989, 1991, and 1996, respectively.

In 1991, he joined the faculty of Engineering at Hokkaido University. Since 1998, he has been with the faculty of Engineering at Niigata University, Niigata, Japan, where he is currently an Associate Professor in the Biocybernetics Engineering Department. His current interests are in the area of small antenna, planar antenna, millimeter antenna, antenna analysis, antenna measurement, and electromagnetic compatibility.

Dr. Ishii is a member of the IEICE of Japan.

Michio Miyakawa (M'86) was born in Gunma Prefecture, Japan, in 1947. He received the D.Eng. degree from Hokkaido University, Sapporo, Japan, in 1977,

He joined the Electrotechnical Laboratory, Japanese Agency of Industrial Science and Technology (AIST), MITI, Tsukuba, Japan, in 1977, where he became a Senior Research Scientist in 1982 and worked on infrared- or microwave-thermometry in addition to organizing the National Project by MITI on the development of hyperthermia equipment for cancer treatment. In 1991, he was appointed Professor at the Faculty of Engineering, Niigata University, Niigata, Japan, where he has been involved in research programs relating to noninvasive thermometry using microwaves, methods of three-dimensional local SAR measurement and observation, themes on human interface, and so on. Currently, he is a Professor of the Center for Transdisciplinary Research at the university. From 1995 to 1996, he was a Visiting Scientist at the Central Institute for Biomedical Engineering, University of Ulm, Ulm, Germany, where he was involved in a research project for developing the hyperthermia system.

Dr. Miyakawa is a member of the IEICE, IEE of Japan, Japanese Society of ME and BE, Information Processing Society of Japan, Society of Instrument and Control Engineers, and Japanese Society of Hyperthermic Oncology.

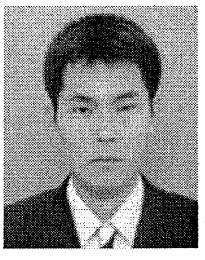

Koji Sakai was born in Shiozawa, Niigata Prefecture, Japan, in 1977. He received the B.S. and M.S. degrees from Niigata University, in 2000, and 2002, respectively.

He is currently an Engineer with Advantest Corporation, Tokyo, Japan. As a graduate student of Niigata University, he worked on new electromagnetic compatibility material development.